Vol. 40 (2009) *ACTA PHYSICA POLONICA B* No 3

THEORY OF NUCLEAR STABILITY USING POINT GROUP SYMMETRIES: OUTLINE AND ILLUSTRATIONS*

J. Dudek[a], K. Mazurek[b], D. Curien[a], A. Dobrowolski[c]
A. Góźdź[c], D. Hartley[d], A. Maj[b], L. Riedinger[e], N. Schunck[e]

[a]IPHC/DRS Université de Strasbourg
23, rue du Loess B.P.28, F-67037 Strasbourg Cedex 2, France
[b]H. Niewodniczański Institute of Nuclear Physics PAN
Radzikowskiego 152, 31-342 Kraków, Poland
[c]Zakład Fizyki Matematycznej, Uniwersytet Marii Curie-Skłodowskiej
pl. Marii Curie-Skłodowskiej 1, 20-031 Lublin, Poland
[d]Department of Physics, U.S. Naval Academy, Annapolis, MD 21402, USA
[e]Dept. of Physics and Astronomy, Univ. of Tennessee, Knoxville, TN 37996, USA

(Received November 26, 2008)

We present what we call *a new theory of nuclear stability* enabled by the combination of the realistic nuclear mean-field and the group theory approaches. It allows us to simplify searches for the strong quantum shell effects at nuclear shapes that result from spectral properties deduced from group theory and geometrical symmetries rather than through 'brute force numerical search'. Illustrations are presented and discussed.

PACS numbers: 21.60.–n, 21.10.–k

1. Introduction

In this article we formulate and illustrate general criteria connecting geometrical symmetries of nuclei and the implied nuclear stability. The approach is based on the group-theory analysis of geometrical symmetries of the mean-field nuclear Hamiltonian. The formulation includes previous discussions of nuclear stability using the D_{2h}^D and D_{∞}^D-symmetries of the triaxial harmonic oscillator[1] introduced by the Copenhagen group as partic-

* Presented at the Zakopane Conference on Nuclear Physics, September 1–7, 2008, Zakopane, Poland.

[1] We refer to axial (D_{∞}^D-symmetric) and tri-axial (D_{2h}^D-symmetric) harmonic oscillator potentials with the frequency ratios $\omega_x : \omega_y : \omega_z = k : m : n$ as criterion for maximizing the gaps and level degeneracies, k, m and n being small integer numbers. Group-theory generated criteria are discussed below in a more general context.

ular cases, and extends the discussion of Ref. [1]. By formulating the general group-theoretical approach, we hope to address the research areas of stable (in the nuclear scale), usually excited nuclear configurations that remain so far undiscovered or poorly explored.

In the following we keep our considerations general by adopting only two very well accepted and so far among the two most successful strategies:

- We assume validity of the nuclear mean-field theory, combined with:
- The use of the group and group representation theories.

Such a strategy implies directly the possibility of using realistic approaches, *e.g.*, nuclear Hartree–Fock or Hartree–Fock–Bogliubov theories, as well as phenomenological realisations of such theories that include the relativistic approaches based on the nuclear mean-field concept. As a consequence, the comparison with experiments become possible from the very beginning; it will remain one of our primary goal here.

2. Nuclear mean-field and the principles of the new theory of nuclear stability

As it is well known, saturation properties of the nuclear forces imply that the depth of the nuclear mean-field potential, V_0, is nearly constant, *i.e.*, approximately independent of the nuclear mass. It then follows, that the average level spacing, $\langle d \rangle \approx V_0/N_b$, where N_b denotes the number of bound levels $\{e_n;\, n = 1, 2, \ldots\, N_b\}$ in the mean-field potential well. So defined average level spacing gives merely an orientation about the order of magnitude, since the density of levels increases when the level-energy e_n gets farther and farther away from the bottom of the potential well, $V_0 \approx -60$ MeV. This trend is quantitatively illustrated in Fig. 1 based on the traditional spherical harmonic oscillator. Indeed, on the first excited level at $\hbar\omega_o$ at most two particles can be placed, while at the $6^{\rm th}$ harmonic oscillator shell already 112 particles can participate in the excited spectrum; N_b increases super-linearly with the nuclear mass. The huge degeneracies seen in the oscillator spectrum are partially an artifact of the so-called accidental degeneracy of various ℓ-levels within a given main shell, *cf.* Fig. 1.

In more realistic situations corresponding, *e.g.*, to phenomenological finite deformed Woods–Saxon and/or Yukawa-folded potentials, the accidental ℓ-degeneracies do not appear anymore, but still the leading factor in a search for particularly stable nucleonic configurations is equivalent to the search for the largest possible gaps in the single particle spectra.

General symmetry arguments are based on the well known properties of the group-symmetric Hamiltonians that can be formulated as follows. Let $G \equiv \{g_1, g_2, \ldots\, g_f\}$ be a symmetry group of the mean-field Hamiltonian

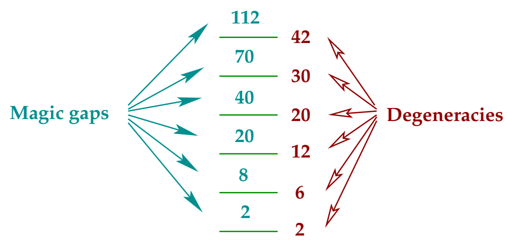

Fig. 1. Single-particle spectrum of the spherical harmonic oscillator. Extreme degeneracies are caused partially by the spherical symmetry [SO(3)-group] but also by the fact that the H.O.-Hamiltonian is invariant under the larger, SU(3)-group, causing 'accidental' ℓ-orbital degeneracy within a given (main) shell N.

H, which implies that $\forall\ g_k \in G$ we have $[H, g_k] = 0$. Let G have r irreducible representations with dimensions $d_1, d_2\ \ldots\ d_r$. Then the eigen-values of the Hamiltonian will split into as many families as there were irreducible representations, while within each family all the levels will form degenerate sub-sets (multiplets) with degeneracies equal to the dimensions of the irreducible representations, Ref. [2]. The above general property has several consequences for the mean-field Hamiltonians of Fermions and below we formulate some relevant comments.

The groups of interest here are: the continuous spherical symmetry group SO(3) and groups representing axial symmetries C_∞^D and D_∞^D as well as finite, discrete point-groups very well known from molecular physics. By definition, the latter ones leave at least one point of the considered object invariant. In the case of Fermion systems these groups must have slightly modified structure as compared to the 'traditional' molecular prototype point-groups in that they assure the fundamental transformation property for the Fermions: $R(2\pi)\psi = -\psi$, where $R(2\pi)$ is an arbitrary-axis rotation about the angle of 2π. Such modified groups are called 'double', *cf.* Ref. [3]; they are denoted with the superscript D, as, *e.g.*, T_d^D for the tetrahedral group, see below.

It can be demonstrated that the irreducible representations of all the double point groups describing symmetries of non-spherical systems are equal either to 2 or to 4 [compared with $(2j+1)$ for spherical symmetry]. There are only 3 symmetry point groups that can be applied to deformed nuclei and which generate 4-fold degeneracies of the nuclear mean-field, *viz.*, tetrahedral T_d^D, octahedral O_h^D, and icosahedral[2] Y_h^D point groups. Thus there is

[2] Tetrahedron is the simplest Platonic polyhedron with four equilateral triangular faces, octahedron has eight such faces, and icosahedron 20. It has been shown, see Refs. [5–8], that the symmetries generated by the first two polyhedra may lead to very strong shell structures in nuclear physics applications; the latter was not investigated but is believed to be 'too close' to the spherical symmetry to provide genuinely new structures in the nuclear context.

only a very small number of symmetries that provide the *four-fold degenerate multiplets*, the analogues of the $(2j+1)$-degenerate multiplets of spherical symmetry — all other double point groups implying only the Kramers (double — or — spin-up/spin-down) degeneracies for non-spherical nuclei. This is also why tetrahedral and octahedral symmetries have been examined as the first candidates of the possible nuclear exotic symmetries.

Let us consider mean-field Hamiltonian H and its group of symmetry G having r irreducible representations. Single-particle levels belonging to a given representation never cross[3] according to the very well-known *Landau–Zener non-crossing rule*. Realistic calculations demonstrate that the single-particle levels have a tendency to fill-in the available energy window defined by the potential depth V_0 (*cf.* the schematic illustration in Fig. 2). These levels are said to 'repel each other', the 'repulsion' leading occasionally to very large gaps in the spectra. Superposition, illustrated schematically on

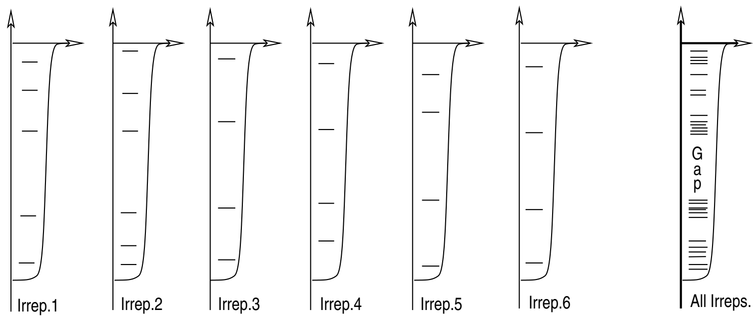

Fig. 2. Consider a symmetry point-group with six irreducible representations (this is actually the case of the octahedral group). The single-particle levels are split into six families, see text, to each of which the Landau–Zener non-crossing rule applies.

the right-hand side of Fig. 2, of the levels belonging to all the irreducible representations often produces a final result with very large gaps 'surviving' in the spectra and thus leading to an increased nuclear stability. This is the central argument of our formulation (qualitative at this point) of the principles of the new theory of nuclear stability. Interested reader may consult Ref. [9], Figs. 3–4, for the illustration of large gaps corresponding to tetrahedral symmetry in the rare-earth and actinide nuclei, see also examples below.

[3] The discussed property is not a theorem (exceptions may occur) and this is why it is referred to as Landau–Zener *rule*. However, accidental symmetries that may lead to such crossings are extremly rare in realistic situations of interest here. The interested reader may consult Ref. [4] and references therein.

Let us stop for a few technical observations at this point. As it is well known from mathematics, some groups possess pairs of complex one-dimensional irreducible representations that are complex conjugates. Such pairs can be equivalently expressed in terms of the real two-dimensional irreducible representations — one of the mechanisms behind the Kramers' spin-up/spin-down degeneracies whose mathematical foundation comes from the Wigner theorem. Such a mechanism must necessarily be present in the spectra of time-independent spinor Hamiltonians — the case of interest here. For example, group C_{6h}^D (*cf.* Table I, which has $\mathcal{N} = 12$ one-dimensional complex-conjugate irreducible representations appears, from the degeneracy point of view, as a group equivalent to the one with $\mathcal{N}/2 = 6$ real 2D representations thus leading to six families of double degenerate levels. This property is marked in Table I with the bar symbol over the Type label.

TABLE I

Symmetry pointgroups whose numbers of irreducible representations are larger than those of the *reference*: the well-known D_{2h}^D triaxial nuclear symmetry defined in terms of the quadrupole deformations (β, γ). The third column defines the conventional 'type' of symmetry — a label used in the text; the fourth column gives the numbers of irreducible representations belonging to each group.

No.	Group	Type	No. Irr.	Dimensions
1	O_h^D	A	6	$4 \times$ 2D and $2 \times$ 4D
2	T_d^D	A	3	$2 \times$ 2D and $1 \times$ 4D
3	C_{6h}^D	$\overline{B}$	12	$12 \times$ 1D ($6 \times$ 2D)
4	D_{6h}^D	B	6	$6 \times$ 2D
5	C_{4h}^D	$\overline{C}$	8	$8 \times$ 1D ($4 \times$ 2D)
6	D_{4h}^D	C	4	$4 \times$ 2D
7	D_{3h}^D	D	3	$3 \times$ 2D
8	C_{6v}^D	D	3	$3 \times$ 2D
9	D_6^D	D	3	$3 \times$ 2D
10	C_6^D	$\overline{D}$	6	$6 \times$ 1D ($3 \times$ 2D)
11	S_6^D	$\overline{D}$	6	$6 \times$ 1D ($3 \times$ 2D)
12	C_{3h}^D	$\overline{D}$	6	$6 \times$ 1D ($3 \times$ 2D)
13	C_{3i}^D	$\overline{D}$	6	$6 \times$ 1D ($3 \times$ 2D)
14	D_{2h}^D	X	2	$2 \times$ 2D (reference)

The properties of irreducible representations underlying the criteria of nuclear stability are listed in Table I. The names of the symmetry groups are given in the second column; the third column gives a label called 'Type'. Groups of the Type A have either one or two four-dimensional irreducible representations, Type B have 6-, Type C have 4-, and finally Type D have 3 two-dimensional irreducible representations. Groups denoted as Type $\overline{B}$, $\overline{C}$, and $\overline{D}$ have $\mathcal{N}$ two-dimensional real representations ($\mathcal{N} = 6, 4$, and 3 as in the case for the groups B, C, and D, respectively) equivalent to $2\mathcal{N}$ complex, one-dimensional ones. According to our global criteria presented above, each of the groups listed in the Table has potentially more capacity of generating gaps larger than the ones known from the properties of triaxial nuclei, *i.e.* 'by the usual' D_{2h}^{D} symmetry group here considered as reference.

Let us emphasize that what we refer to as *symmetry criteria for large gaps and thus increased nuclear stability* are merely strategical guidelines for advanced realistic calculations — such calculations are illustrated below.

3. Tetrahedral symmetry and competition between symmetries

The most often studied shapes of deformed nuclei correspond to axial symmetry, either with the dominating α_{20} and α_{40} quadrupole and hexadecapole deformations, respectively, or with an extra α_{30} pear-shape component referred to as octupole[4]. We will be able to present merely a few selected examples of the exotic-shape symmetries; we will focus on the competition between the 'traditional' and new symmetries.

To begin, let us first emphasize a big difference between the spherical symmetry and related magic numbers and the exotic symmetries together with their implied magic numbers: while the former corresponds to the one and only, well defined (*viz.* spherical) shape, the latter generate in general an infinity of shapes[5]. Performing systematic mean-field calculations, one can obtain a series of magic numbers that characterize each exotic symmetry with a series of associated characteristic deformations. Calculated tetrahedral magic numbers are $30, 40, 56, 64, 70, 90, 112, 136$.

Below we selected a combination of three tetrahedral neutron magic numbers, *i.e.*, $N = 40, 56$, and 70 with the proton magic number $Z = 40$ (zirconium). Comparison shows[6] that the axial-symmetric pear-shape type

---

[4] In the present context we have four distinct octupole shape possibilities related to the surfaces represented by Y_{30}, $(Y_{3,+1} - Y_{3,-1})$, $(Y_{3,+2} + Y_{3,-2})$, and $(Y_{3,+3} - Y_{3,-3})$.

[5] There is no spherical shape 'more spherical than the other one' — but some nuclei may have larger tetrahedral deformation as compared to the neighbours.

[6] We use here the macroscopic–microscopic method with the Yukawa-folded realisation as the 'macro'- and the universal-compact Woods–Saxon parameterisation version for the 'micro'-terms, *cf.* Ref. [8] and references therein.

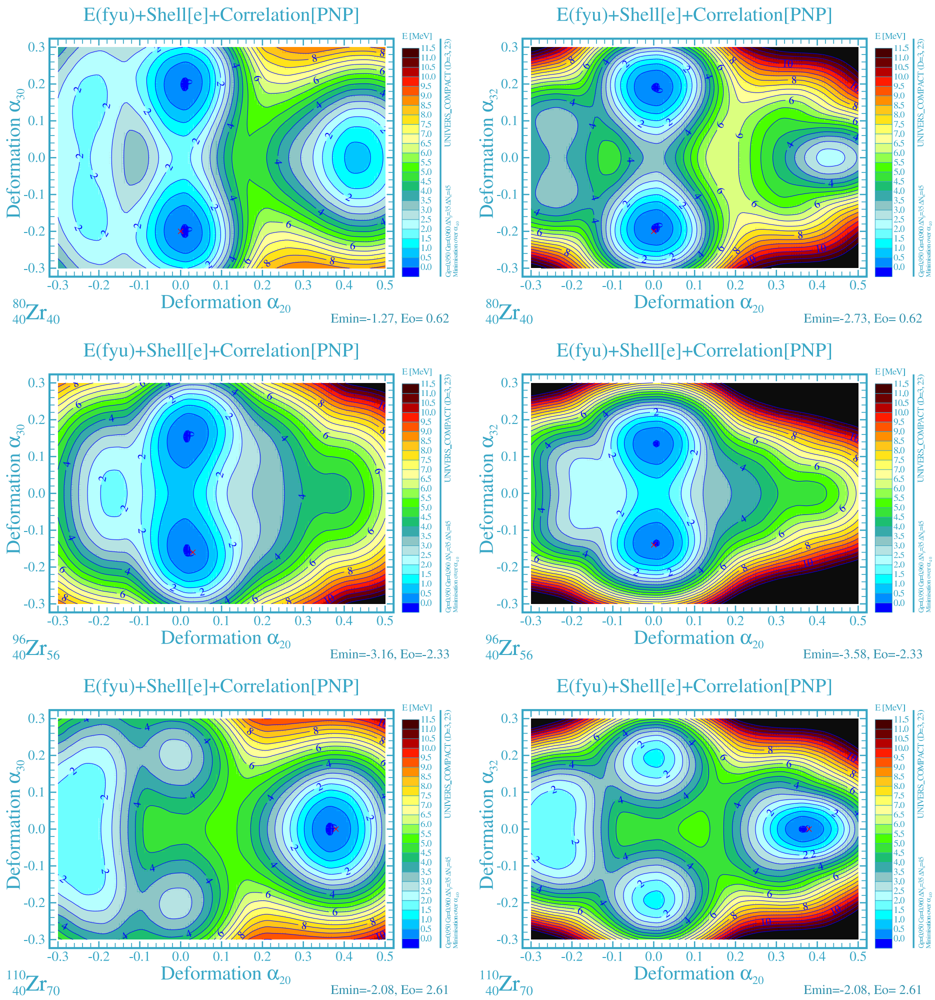

Fig. 3. Total energy surfaces with the axial-octupole deformation (left) and tetrahedral-symmetric deformation (right) plotted *versus* quadrupole deformation.

octupole minima are in a competition with the tetrahedral symmetry minima, as illustrated in Fig. 3. We note that the tetrahedral symmetry wins the competition in all the three considered cases.

The case of ^{96}Zr deserves particular attention, since it is usually referred to as a 'good spherical shell-model nucleus'. The illustration in Fig. 3 implies, however, that the spherical shape for this nucleus is certainly unstable by at least 3 MeV (!) — and there is no other minimum, *e.g.*, quadrupole-deformed, in this nucleus. Calculations presented here suggest therefore

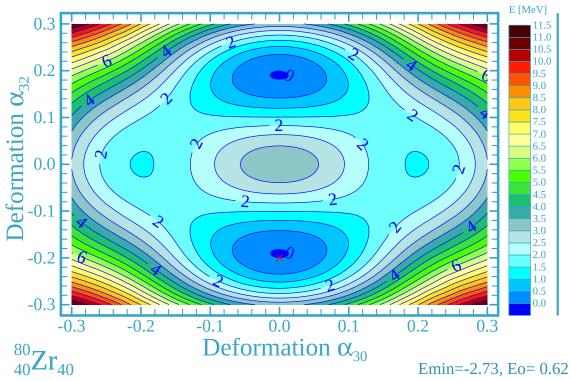

Fig. 4. Competition between the pear-shape octupole (horizontal axis) and tetrahedral or triaxial-octupole (vertical axis); tetrahedral minimum lies lower by about 1.5 MeV. The landscapes for the other two tetrahedral-magic zirconium nuclei are very similar.

that ^{96}Zr is tetrahedral deformed *in its ground state*. Moreover, experiment shows one of the strongest B(E3) values ever measured — in this particular nucleus.

Is it possible to combine these two apparently contradicting situations into a one coherent scenario? We believe that there exists such a possibility. First of all, ^{96}Zr, like every even–even nucleus, has $I^\pi = 0^+$ in the ground state and must appear to the outside world as a spherical object. The lowest-lying particle–hole excited states will lead to the j^2- or (j_1, j_2)-configurations coupled with the remaining even–even $(A-2)$ nuclear 'core', the latter again with a 0^+ configuration leading to the structures of the type $(j_1 \otimes j_2 \otimes 0^+)_{J^\pi}$. Such structures will provide spin sequences that resemble irregular energy *vs.* spin sequences observed in many nearly spherical nuclei with a few excited particles. The same will necessarily happen in the low-lying excitations of ^{96}Zr manifesting the spherical[7] structure — *independent* of the underlying

[7] It is perhaps worth alerting the reader at this point that the word 'spherical shape' is, strictly speaking, largely abused. First of all, only the ground states of doubly magic (traditional sense) nuclei can be considered really spherical. In reality, each particle–hole excitation generates a polarisation that is accompanied by a comparable polarisation of the remaining nuclear bulk. Secondly, any few-particle–hole configuration of the structure $(j_1 \otimes j_2 \otimes \ldots 0^+)$ will hide the actual geometry of the remaining 0^+ core, thus rendering it invisible from the spectra.

actual geometrical shape[8] of this nucleus. Within mean-field interpretation it is the 0^+ configuration that carries the tetrahedral symmetry information and consequently remains disguised as long as there is no extra evidence, *e.g.*, in the form of a collective tetrahedral rotational band. Here, however, comes another fascinating challenge related to this type of (new) physics: within the exact tetrahedral symmetry the rotational bands do not generate intra-band E2 transitions, thus rendering *the detection* of the structure in question certainly more difficult, although definitely not impossible. We believe that ^{96}Zr represents an important challenge — in fact encouraged by experiment: the $B(\mathrm{E3}) = 57(4)$ W.u. — one of the largest seen so far, *cf.* Ref. [10]; the possibility of an existence of tetrahedral effects in the Zirconium region has attracted already attention of theorists using the Generator Coordinate Method together with Hartree–Fock and projections techniques, *cf.* Ref. [11].

4. Electromagnetic transitions: possible probe of symmetry competition

Examining the electromagnetic properties of nuclei with the tetrahedral symmetry is considered to be one of the most promising tools for possible unambiguous confirmation of the presence of such nuclei in nature. However, exact tetrahedral symmetry implies vanishing of the quadrupole moments within the tetrahedral bands and therefore vanishing of the intra-band E2 transitions. On the other hand, there exist reasons for a partial breaking of such a symmetry:

a. the zero-point quadrupole and octupole oscillations;

b. the Coriolis (rotational) alignment of angular momenta;

c. shape evolution (closing the tetrahedral gaps) with increasing spin;

d. the presence of valence nucleons on top of the tetrahedral magic gaps.

Here we would like to address in particular the problem of the zero-point motion, one of the most evident and long-time known quantum mechanisms that is not so often receiving the attention that it deserves. In the mass $A \sim 150$ nuclei we obtain an estimate of the dynamical (the most probable) deformation by using the stiffness coefficients extracted from our microscopic

[8] The arguments here are similar to the one of N. Bohr who remarked that even though there may be majority of even–even nuclei that are deformed in their ground-states, as long as they are not excited they must manifest the spherical symmetry. Here it is the non-excited $(A-2)$ core that plays a similar role.

total energy calculations and a phenomenological estimate of the mass parameters; the resulting most-probable deformation varies typically between 0.04 and 0.09 or so. As the next step we use the deformations of this order of magnitude to obtain the microscopic *transition* multipole moments $Q^{\rm micro}_{\lambda\mu}$ for the quadrupole and octupole motions and next the reduced transition probabilities $B(\mathrm{E2})$ and $B(\mathrm{E1})$. This is done by using the Slater determinants constructed out of the single-particle wave functions calculated using the phenomenological deformed Woods–Saxon Hamiltonian.

TABLE II

Calculated ratios of the reduced transition probabilities, B(E2) from 15^- to 13^- within the 'tetrahedral' sequence in ^{156}Gd (*cf.* Fig. 4 of Ref. [8]) compared to inter-band transitions from $I^\pi = 15^-$ of the tetrahedral to the 14^+ of the ground-state band in the same nucleus. The tetrahedral minimum has been 'contaminated' with small quadrupole deformations simulating the presence of the zero-point motion: $\alpha_{20} = 0.04$ for three triaxialities represented by $\gamma^t = 0°$ (small axial quadrupole deformation) together with $\gamma^t = 15°$ and $\gamma^t = 30°$ shown for comparison.

$B(\mathrm{E2})/B(\mathrm{E1}) \times (10^6\mathrm{fm}^2)$			
$\alpha_{30}^{\rm gsb}$	$\gamma^t = 0°$	$\gamma^t = 15°$	$\gamma^t = 30°$
0.08	0.84	0.53	2.61
0.12	0.37	0.36	2.18
0.15	6.19	1.48	3.20
0.18	6.28	4.74	4.70

As the last step we assume the band-mixing picture: the ground-state band (gsb) for which we assume also the presence of the pear-shape octupole zero-point motion and the tetrahedral negative parity band with odd spins, Ref. [12], are mixed with amplitudes $a^2 \sim 0.95$ and $b^2 \sim 0.05$ expected from the Coriolis mixing of the octupole degrees of freedom (recall that tetrahedral deformation is equivalent to a 'triaxial octupole deformation' and thus implies a strong K mixing) as well as from the mixing of single-particle states of opposite parities. We assumed that the ground state has the calculated static deformations $\alpha_{20} = 0.2$ and $\alpha_{40} = 0.08$; on top of this we test the effect of increasing admixtures of the dynamical axial-octupole vibrations as listed in the first column of Table 2, where the theoretical ratio $B(\mathrm{E2})/B(\mathrm{E1})$ is tabulated. Similarly we assume the dynamical quadrupole deformation $\alpha_{20} \approx 0.04$ for the tetrahedral minimum and propose three hypotheses of $\gamma = 0°, 15°$ and $30°$ to obtain a typical variation of our observable as a function of the most relevant dynamical deformation parameters. The results are presented in Table II for the $B(\mathrm{E2} : 15^- \to 13^-)/B(\mathrm{E1} : 15^- \to 14^+)$ transitions. The corresponding results are expected to grow with spin, due to Coriolis polarisation an in principle we should have recalculated the multipole moments for the increasing spins using *e.g.* the cranking model. In this preliminary calculation aiming at the order-of-magnitude estimates we kept the multipole moments constant. The recent experimental results from Ref. [12] give the values of $5.5 \times (10^6\ \mathrm{fm}^2)$ and $4.5 \times (10^6\ \mathrm{fm}^2)$ for spins 13^- and 15^-, respectively, the results which are slightly higher than, but close to our calculated values.

The calculated values, here obtained without taking into account the pairing effect, vary from one deformation point to another but remain of the right order of magnitude. Given the fact that we have used the technique of Slater determinants built out of the realistic microscopic mean-field wave functions we may consider this result encouraging. It is expected that taking into account the pairing should diminish the fluctuations while taking into account the quadrupole-moment polarisation as the result of Coriolis effect should contribute to increasing, on the average, the calculated $B(\mathrm{E2})/B(\mathrm{E1})$-ratio with increasing spin.

5. Summary and conclusions

We have formulated the global criteria of nuclear stability based on the assumption that the nuclear stability increases with the increase of the gaps in the nucleonic single-particle spectra. According to the group theory arguments, the geometrical symmetries whose point groups have a relatively large number of irreducible represetations as well as those whose dimensions are possibly high, or both of these properties simultaneously, are the best candidates to generate strong *shell effects*. The strong shell effects alone are not a sufficient condition to obtain stable minima in the total energy surfaces but they a necessary condition. Realistic calculations whose results are used for illustration confirm these general lines of thinking. We illustrated the results for the tetrahedral symmetry group (three irreducible representations out of which one is four-dimensional).

Finally we present the first order-of-magnitude theoretical estimates for the observable ratio $B(\mathrm{E2})/B(\mathrm{E1})$; recent experiments confirm that one should expect the result of the order of $\sim 5 \times 10^6\ \mathrm{fm}^2$ for $\mathrm{I} > 11$; a very similar order of magnitude result has been obtained with our preliminary calculations using the zero-point motion and the band-mixing concepts.

This work was partially supported by the Collaboration TetraNuc through the $\mathrm{IN_2P_3}$, France, through the exchange program between $\mathrm{IN_2P_3}$, France, and Polish COPIN nuclearphysics laboratories and by the Polish Ministry of Science and Higher Education (Grant 1 P03B 030 30 and N N 202 309135).

REFERENCES

[1] J. Dudek, J. Dobaczewski, N. Dubray, A. Góźdź, V. Pangon, N. Schunck, *Int. J. Mod. Phys.* **E16**, 516 (2007).

[2] J.F. Cornwell, *Group Theory in Physics*, Academic Press 1984, Volume I, Part A, Chapter I-4, p. 21 (Theorem I).

[3] *cf.* Ref. [2], Part A, Chapter VI-4, p. 21 (Theorem VII).

[4] J. Von Neumann, E. Wigner, *Phys. Z.* **30**, 467 (1929); *cf.* also: K. Razi Naqvi, W. Byers Brown, *Int. J. Quant. Chem.* **6**, 271 (1972); G. Hatton, *Phys. Rev.* **A14**, 901 (1976); K. Razi Naqvi, *Phys. Rev.* **A15**, 1807 (1977).

[5] X. Li, J. Dudek, *Phys. Rev.* **C49**, 1246 (1994).

[6] J. Dudek, A. Góźdź, N. Schunck, M. Miśkiewicz, *Phys. Rev. Lett.* **88**, 252502 (2002).

[7] N. Schunck, J. Dudek, A. Góźdź, P.H. Regan, *Phys. Rev.* **C69**, 061305 (2004).

[8] J. Dudek, D. Curien, N. Dubray, J. Dobaczewski, V. Pangon, P. Olbratowski, N. Schunck, *Phys. Rev. Lett.* **97**, 072501 (2006).

[9] J. Dudek, A. Góźdź, N. Schunck, *Acta Phys. Pol. B* **34**, 2491 (2003).

[10] D. Abriola, A.A. Sonzogni, *Nucl. Data Sheets* **109**, 2501 (2008).

[11] K. Zberecki, P. Magierski, P.-H. Heenen, N. Schunck, *Phys. Rev.* **C74**, 051302(R) (2006); K. Zberecki, P.-H. Heenen, P. Magierski, *Int. J. Mod. Phys.* **E16**, 533 (2007).

[12] Q.T. Doan *et al.*, *Acta Phys. Pol. B* **40**, 725 (2009) these proceedings.